European Journal of Cardio-Thoracic Surgery 50 (2016) 955–961
doi:10.1093/ejcts/ezw180 Advance Access publication 30 May 2016

ORIGINAL ARTICLE

Cite this article as: Nauta FJH, Conti M, Marconi S, Kamman AV, Alaimo G, Morganti S *et al*. An experimental investigation of the impact of thoracic endovascular aortic repair on longitudinal strain. Eur J Cardiothorac Surg 2016;50:955–61.

An experimental investigation of the impact of thoracic endovascular aortic repair on longitudinal strain†

Foeke J.H. Nauta[a,b,*], Michele Conti[c], Stefania Marconi[c], Arnoud V. Kamman[a,b], Gianluca Alaimo[c], Simone Morganti[d], Anna Ferrara[c], Joost A. van Herwaarden[b], Frans L. Moll[b], Ferdinando Auricchio[d] and Santi Trimarchi[a]

[a] Thoracic Aortic Research Center, Policlinico San Donato IRCCS, University of Milan, Italy
[b] Department of Vascular Surgery, University Medical Center Utrecht, the Netherlands
[c] Department of Civil Engineering and Architecture, Beta-lab, University of Pavia, Italy
[d] Department of Industrial Engineering and Informatics, University of Pavia, Italy

* Corresponding author. Thoracic Aortic Research Center, Policlinico San Donato IRCCS, University of Milan, Piazza Malan 2, 20097 San Donato Milanese, Milan, Italy. Tel: +39-02-52774344; fax: +39-02-52774383; e-mail: foekenauta@gmail.com (F.J.H. Nauta).

Received 17 February 2016; received in revised form 15 April 2016; accepted 26 April 2016

Abstract

OBJECTIVES: To investigate the impact of thoracic endovascular aortic repair (TEVAR) on longitudinal strain and assess aortic tensile properties in order to better understand complications associated with TEVAR.

METHODS: Twenty fresh thoracic porcine aortas were harvested and connected to a mock circulatory loop driven by a centrifugal flow pump at body temperature. Length measurements were conducted before and after TEVAR through aortic marking, high-definition imaging and custom-developed software under physiological pressure conditions (i.e. between 100 and 180 mmHg with 20 mmHg increments). Longitudinal strain was derived from length amplitude divided by the baseline length at 100 mmHg. Three groups of stent-graft oversizing were created (0–9, 10–19 and 20–29%). Finally, elastic properties of the aortic samples were assessed in both longitudinal and circumferential directions through uniaxial tensile testing. Longitudinal strain was compared before and after TEVAR, and stress-to-rupture was compared among specimens and locations.

RESULTS: TEVAR induced a longitudinal strain decrease from 11.9 to 5.6% ($P < 0.001$) in the stented segments and a longitudinal strain mismatch between stented (5.6%) and non-stented segments (9.1%, $P < 0.001$). Stent-graft oversizing did not affect the magnitude of strain reduction ($P = 0.77$). Tensile testing showed that peak stress-to-rupture was lower for longitudinal (1.4 ± 0.4 MPa) than for circumferential fragments (2.3 ± 0.4 MPa, $P < 0.001$). In addition, longitudinal fragments were more prone to rupture proximally than distally ($P = 0.01$).

CONCLUSIONS: This experimental study showed that TEVAR acutely stiffens the aorta in the longitudinal direction and thereby induces a strain mismatch, while tensile testing confirmed that longitudinal aortic fragments are most prone to rupture, particularly close to the arch. Such an acute strain mismatch of potentially vulnerable tissue might play a role in TEVAR-related complications, including retrograde dissection and aneurysm formation. The finding that TEVAR stiffens the aorta longitudinally may also shed light on systemic complications following TEVAR, such as hypertension and cardiac remodelling. These observations may imply the need for further improvement of stent-graft designs.

Keywords: Aortic strain • Stent-graft • Thoracic aorta • TEVAR • Uniaxial tensile testing

EXPERIMENTAL

INTRODUCTION

The use of thoracic endovascular aortic repair (TEVAR) is increasing rapidly, even in younger patients [1, 2]. However, this procedure is associated with serious complications such as retrograde dissection (with a mortality of about 40%), aneurysm formation, stent-graft induced new entry tears and rupture [3–5]. These complications might be related to different physical properties of the stent-grafts when compared with blood vessels. Current stent-grafts are several orders of magnitude stiffer than the native aorta [6, 7], most notably in the longitudinal axis. Their impact on the cardiovascular system remains unclear. Locally, segmental aortic stiffening seems to increase wall stress in segments adjacent to the stent-graft due to a compliance mismatch [3]. This has been

† This study has been done at the Thoracic Aortic Research Center, Policlinico San Donato IRCCS, University of Milan, Italy, in collaboration with the Department of Civil Engineering and Architecture, Biomechanics for Endovascular Treatments of the Aorta (Beta-lab), University of Pavia, Italy and the Department of Vascular Surgery, University Medical Center Utrecht, Netherlands.

associated with reduced wall strength and subsequent complications [3–5]. Stent-graft oversizing reduces aortic wall strength even further [8].

In addition to a local impact, TEVAR might affect the cardiovascular system on a systemic level. In this setting, aortic elasticity serves a critical function in damping the highly pulsatile flow coming from the left ventricle [9], known as the 'Windkessel effect' [10]. Stiffening of the thoracic aorta diminishes this effect with major implications for cardiovascular disease development as it increases cardiac afterload and decreases coronary perfusion [11, 12]. It has been reported that TEVAR stiffens the aorta acutely, resulting in hypertension and cardiac remodelling in the early and late phase [2, 13]. This phenomenon may be referred to as cardiovascular remodelling and might determine long-term outcomes of TEVAR.

Aortic strain is an established measure of aortic elasticity and is traditionally reported as deformation in the circumferential direction during a cardiac cycle. This seems to diminish after abdominal endovascular repair [14]. However, aortic tissue is more prone to rupture in the longitudinal axis [15] and most intimal tears are circumferentially orientated due to the increased longitudinal stress [16].

The aim of this study was, therefore, to assess the impact of TEVAR on longitudinal strain in a controlled experimental setting, with also attention to the role of stent-graft oversizing. For this purpose, we used an *ex vivo* porcine aortic model connected to a mock circulatory loop driven by a centrifugal flow pump, quantifying changes of longitudinal strain for increasing pressure, before and after TEVAR. In addition, we used uniaxial tensile testing to study stress-to-rupture mechanical properties of the aortic specimens, in both circumferential and longitudinal directions, to potentially identify vulnerable aortic segments.

MATERIALS AND METHODS

Preparation of aortas

Twenty fresh porcine aortas were harvested at a local slaughterhouse from young healthy Goland pigs (commercial hybrid, 10–12 months, 160–180 kg). No pigs were sacrificed solely for this study. The thoracic aortas were transported on iced 0.9% saline solution and all experiments were conducted within 12 h from death. The aortas were procured from the origin of the left subclavian artery (LSA) to the origin of the coeliac trunk and all side branches were ligated. Subsequently, the aortas were bathed in 0.9% saline of room temperature for 15 min.

Experimental set-up

The prepared aortas were connected to a mock circulatory loop driven by a centrifugal flow pump (Medtronic Bioconsole BIOMEDICUS 550, Minneapolis, MN, USA), which allowed for controlled intraluminal pressurization. Water was used that was constantly heated at body temperature using a liquid heater (Nova Powerstat Protonic®, Boise, ID, USA) to preserve the biomechanical characteristics of the nitinol stents [17]. A pressure sensor (Micro Switch Pressure Sensor 40PC Series Chart, Honeywell, Freeport, IL, USA) was coupled to a 1/2-inch silicon tube just proximal to the connection with the aorta. The distal end of the aorta was connected to a 3/8–3/8-inch tube, which could move against low resistance in the longitudinal direction through a guiding half-pipe (Fig. 1). The distal 3/8-inch silicon tube was fixed at a standard appointed location to ensure similar resistance and prestretch for all aortas. A prestress of 100 mmHg was applied for all aortas prior to diameter and length measurements, which simulates mean aortic blood pressure in pigs [18].

Measurements of aortic dimensions and longitudinal strain

Baseline diameters and lengths were measured manually, using an electronic calliper and were repeated twice by the principal investigator and twice by a second investigator, to allow for intra- and interobserver variability analysis. Medtronic Valiant stent-grafts (Medtronic Vascular, Santa Rosa, CA, USA) were used and therefore aortic diameter was based on the distance from adventitia to adventitia, as advised by the manufacturer. To capture longitudinal strain, black rubber dots with a diameter of 5 mm were sutured to the superficial adventitia along the anterior side of the aorta, starting at the origin of the LSA followed by every 5 cm distally (Levels L1–L8, Fig. 1). Levels L1 and L8 were excluded from further analysis because they were partly covered by the tube connectors. The segment between L2 and L7 was considered the total aortic length. A high-definition webcam (Logitech HD Pro Webcam C920, Lausanne, Switzerland) was installed and fixed above the aorta and snapshots were conducted at five different pressure moments (i.e. 100, 120, 140, 160 and 180 mmHg). All measurements were

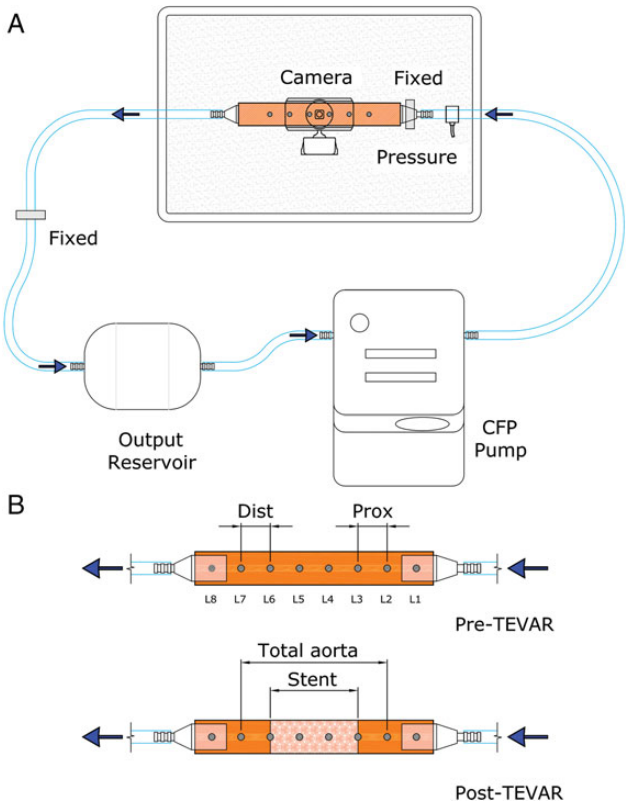

Figure 1: Illustration of the mock circulatory loop connected to a porcine aorta. (**A**) The CFP propels the water through a soft silicon tube into the porcine aorta, with the blue arrow illustrating the direction of flow. 'Fixed' marks the locations where the tube is fixed. 'Pressure' shows the location of the pressure sensor. 'Camera' illustrates the location of the HD-camera. The 'Output Reservoir' is the water reservoir that supplies the CFP. (**B**) 'Pre-TEVAR' shows the situation before TEVAR with the Levels L1–L8 marked accordingly. 'Post-TEVAR' illustrates the situation after TEVAR with 'Stent' marking the stented segments and 'Total Aorta' the total aortic length. The proximal segment adjacent to the stent-graft is marked with 'Prox', while 'Dist' represents the distal adjacent segment. CFP: centrifugal flow pump; TEVAR: thoracic endovascular aortic repair.

conducted in threefold and means were calculated for further analysis. Snapshots were taken at a resolution of 1920 × 1080 pixels. These photos were elaborated by a custom-made program developed with Matlab (The MathWorks©, Inc., Natick, MA, USA) that computed the distance between two consecutive dots through a semiautomatic procedure. The program showed the user each image of the dataset and allowed to select each dot and crop the image. The cropped area was then converted from Red–Green–Blue format to black-and-white format using a fixed threshold. A more precise detection of the centre was then performed using an automatic algorithm, which computed the centre of mass of a black region on a white background. All distances and mean values were exported into a .txt file for analysis. Longitudinal aortic strain was then calculated as

$$\text{Longitudinal strain} = \frac{L - L_0}{L_0}$$

where L is the final length at given pressure and L_0 is the length at baseline (100 mmHg).

Stent-graft implantation

The size of the stent-graft was based on the diameter at the level 10 cm distal to the LSA (Level L3, Fig. 1). To study the impact of circumferential stent-graft oversizing, the aortas were divided into three groups of 0–9% ($n = 7$), 10–19% ($n = 7$) and 20–29% ($n = 6$) of oversizing. Mean longitudinal strains per oversizing group were compared before TEVAR to ensure homogeneity between groups. Medtronic valiant stent-grafts were loaded and deployed by a custom-developed loading and deployment system, directly following the pre-TEVAR measurements. Stent-grafts were implanted with sizes 22–22–150, 24–24–150 or 26–26–150 mm, according to the appointed oversizing rates. The implanted stent-graft extended from the segments between L3 and L6 (Fig. 1). Proximal and distal landing zones were confirmed manually.

Tensile testing

Uniaxial tensile testing was conducted after the experiment to study elastic properties of the porcine aortas. The specimens were preserved in a refrigerator at ∼7°C prior to the tensile testing (time of delay 1.5 ± 0.8 days). Three zones of interest were distinguished in the excised descending thoracic aorta, i.e. proximal, central and distal (Fig. 2A). Both circumferential and longitudinal bone-shaped fragments were cut with a standardized specimen cutter. Tensile tests were performed with the MTS Insight Testing System 10 kN (MTS System Corporation, Eden Prairie, MN, USA) equipped with a 250 N load-cell, and by the ME-46 Video Extensometer (Messphysik, Fürstenfeld, Austria). Peak values of both stress and strain were computed from stress–strain curves recorded during the mechanical testing.

Statistical analysis

Statistical analysis was performed with SPSS statistical analysis software (SPSS 22, Inc., Chicago, IL, USA). Data are shown as frequencies, percentages, mean ± standard deviation, as appropriate. Values identified as outliers by Grubb test ($\alpha = 0.05$) were excluded from the analysis. Shapiro–Wilk test was conducted to

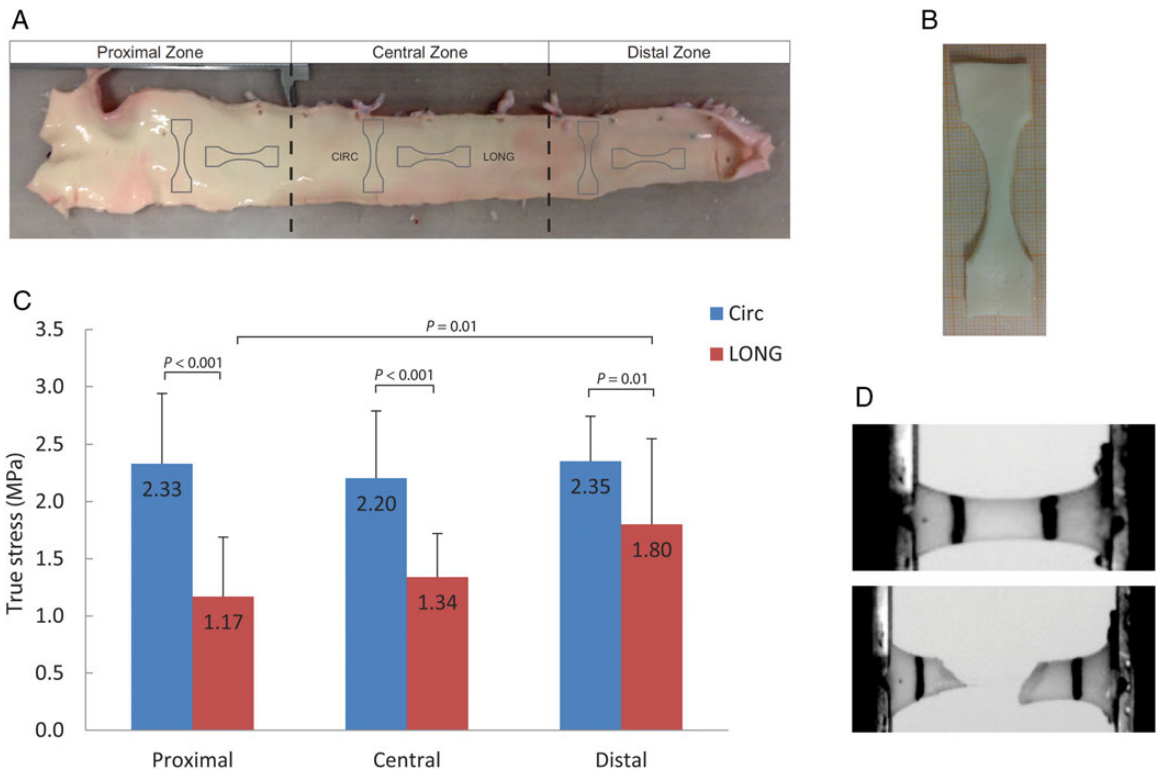

Figure 2: Specimen and results of uniaxial tensile testing. (**A**) Specimen location and orientation. (**B**) Bone-shaped specimens. (**C**) Bar diagrams of aortic mean peak stress-to-rupture as function of zone and orientation. (**D**) Top panel shows aortic specimen under stress. Bottom panel shows rupture of the specimen. Circ: circumferential aortic wall orientation; long: longitudinal aortic wall orientation.

test the normality of data distribution. Statistical significance was evaluated with two-tailed paired *t*-tests, Pearson product–moment correlation or one-way analysis of variance. Repeatability of aortic diameter measurements was analysed with Bland and Altman's difference against mean analysis. Statistical significance was set at the level of $P < 0.05$.

RESULTS

Pre- and post-TEVAR longitudinal strains are presented in Table 1. Time between pre-TEVAR and post-TEVAR measurements was 0.6 ± 0.2 h.

Prethoracic endovascular aortic repair aortic dimensions and longitudinal strain

The mean thoracic aortic length from the LSA to the coeliac trunk was 325.5 ± 29.1 mm and the mean aortic diameter at the level of the proximal landing zone was 20.5 ± 0.9 mm. More detailed aortic dimensions can be found in Supplementary Table 1. Time of delay between harvesting of the aorta and the initiation of the experiment was 7.1 ± 2.6 h and the water temperature was 37.2 ± 0.2°C. Before TEVAR, we observed a significant positive linear correlation between pressure and longitudinal strain ($r = 0.91$, $P < 0.001$). Maximum strains were 11.9% in the prestented segments and 11.4% in the total aorta, observed at 180 mmHg (Fig. 3).

Post-thoracic endovascular aortic repair longitudinal strain

After TEVAR, longitudinal strain between 100 and 180 mmHg decreased in both the stented segments (11.9 vs 5.6%, $P < 0.001$) and the total aorta (11.4 vs 7.0%, $P < 0.001$, Figs 3 and 4). Maximum longitudinal strain of the segment proximal to the stent-graft decreased after TEVAR, while this did not change in the distal segment (Fig. 4). After TEVAR, a mismatch in longitudinal strain was observed between the stented (5.6%) and non-stented adjacent (i.e. proximal plus distal) segments (9.1%, $P < 0.001$, Fig. 5). In addition, the positive linear correlation between longitudinal strain and pressure was reduced after TEVAR at 120 mmHg ($r = 0.86$, $P < 0.001$), and continued to be significant for all higher pressures (Fig. 3).

Table 1: Longitudinal strain as function of pressure per aortic segment

Aortic segment	Pressure (mmHg)	Pre-TEVAR, longitudinal strain (%)	Post-TEVAR, longitudinal strain (%)	*P*-value
Total aorta	100	0.0 ± 0.0	0.0 ± 0.0	–
	120	2.0 ± 0.9	1.4 ± 0.5	0.002
	140	5.1 ± 1.8	3.3 ± 1.2	<0.001
	160	8.5 ± 2.3	5.2 ± 1.9	<0.001
	180	11.4 ± 3.0	7.0 ± 2.6	<0.001
Stented segments	100	0.0 ± 0.0	0.0 ± 0.0	–
	120	2.0 ± 0.9	0.9 ± 0.5	<0.001
	140	5.3 ± 1.7	2.2 ± 1.2	<0.001
	160	8.9 ± 2.3	3.8 ± 1.9	<0.001
	180	11.9 ± 3.1	5.6 ± 2.7	<0.001
Proximal segment	180	9.1 ± 3.9	8.3 ± 3.4	0.02
Distal segment	180	11.8 ± 3.4	10.2 ± 3.6	0.06

Continuous data are presented as the means ± standard deviation.
TEVAR: thoracic endovascular aortic repair.

Oversizing and longitudinal strain

Before TEVAR, homogeneity of longitudinal strain was confirmed between the three stent-graft oversizing groups in the total aorta

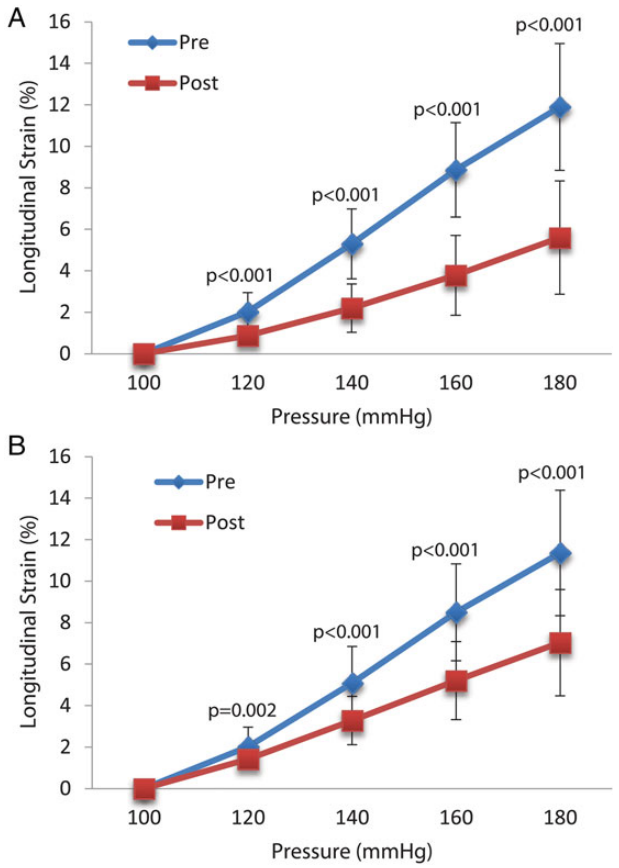

Figure 3: Longitudinal strain as function of pressure. (**A**) Longitudinal strain of the stented segments as function of pressure, pre- and post-TEVAR. (**B**) Longitudinal strain of the total aorta as function of pressure, pre- and post-TEVAR. TEVAR: thoracic endovascular aortic repair.

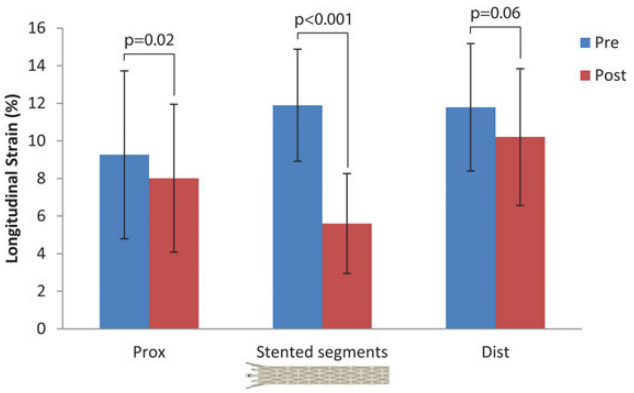

Figure 4: Longitudinal strain per aortic segment, pre- and post-TEVAR. Mean peak longitudinal strain at 180 mmHg per aortic segment. The location of the stent-graft is marked accordingly. Dist: distal segment; Prox: proximal segment; TEVAR: thoracic endovascular aortic repair.

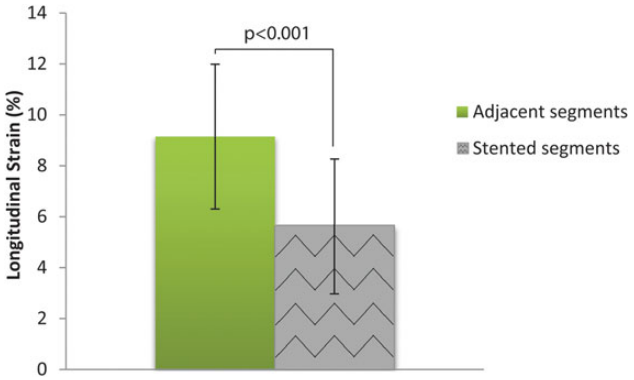

Figure 5: Longitudinal strain mismatch. Post-TEVAR, a mismatch in longitudinal aortic strain is observed between the aortic segments adjacent to the stent-graft compared with the stented segments. TEVAR: thoracic endovascular aortic repair.

Table 2: Longitudinal strain per oversizing group

Aortic segment	Oversizing group (%)	Pre-TEVAR, longitudinal strain (%)	Post-TEVAR, longitudinal strain (%)	*P*-value
Total aorta	0–9	12.3 ± 3.5	7.6 ± 3.3	0.002
	10–19	11.0 ± 2.7	6.7 ± 2.6	0.001
	20–29	10.7 ± 3.0	6.7 ± 1.9	0.001
Stented segments	0–9	12.8 ± 3.5	6.5 ± 3.5	<0.001
	10–19	11.9 ± 2.6	5.4 ± 2.6	<0.001
	20–29	10.9 ± 3.2	4.9 ± 1.8	0.001

Continuous data are presented as the means ± standard deviation.
TEVAR: thoracic endovascular aortic repair.

($P = 0.60$) and in the stented segments ($P = 0.55$). Post-TEVAR, longitudinal strain did not differ significantly between oversizing groups in both the total aorta ($P = 0.77$) and the stented segments ($P = 0.57$, Table 2).

Tensile testing

Following the strain experiments, the aortas were incised along the posterior wall so that the stent-graft could be removed without damaging the aortic tissue of the anterior side. Anterior aortic specimen was then used for uniaxial tensile testing since these fragments were not interrupted by spinal side branches. Figure 2 demonstrates the results of the tensile testing. These data confirmed homogeneity of the aortic mechanical responses among all aortas, with longitudinal and circumferential peak stress-to-rupture of 1.4 ± 0.4 MPa (coefficient of variation = 31.0%) and 2.3 ± 0.4 MPa (coefficient of variation = 16.2%), respectively. Peak stress-to-rupture was significantly lower for the longitudinal than for the circumferential fragments in all three zones (Fig. 2C). Additionally, we found lower stress-to-rupture in proximal longitudinal fragments compared with distal longitudinal fragments ($P = 0.01$), while circumferential fragments showed equal stress-to-rupture in all three zones ($P = 0.61$).

Intra- and interobserver variability

The intraobserver repeatability coefficient (RC) for diameter measurements of observer 1 was 2.45, and 2.01 mm for Observer 2. Differences of the measurements were smaller than the RCs and linear regression analysis was non-significant ($P = 0.46$ and $P = 0.32$, respectively), indicating good intraobserver agreement. The interobserver RC was 1.35 mm. Differences of the measurements between both observers were smaller than the RCs and linear regression analysis was non-significant ($P = 0.06$), indicating acceptable interobserver agreement.

DISCUSSION

This experimental study investigated the impact of TEVAR on longitudinal strain through an *ex vivo* porcine model and assessed stress-to-rupture with uniaxial tensile testing. The experiments were conducted in a controlled environment using fresh porcine thoracic aortas connected to a mock circulatory loop, while creating different groups of stent-graft oversizing.

We observed a significant decrease in longitudinal strain after TEVAR in the stented segments (from 11.7 to 5.6%, $P < 0.001$). As a result, a longitudinal strain mismatch was observed between the stented and non-stented aortic segments. Our observed longitudinal strain before TEVAR was 11.4% between 100 and 180 mmHg. This agrees with a recent study by Krüger *et al.* [19] who found length changes of ∼10% using a similar set-up and with *in vivo* data of Bell *et al.* [20] that showed longitudinal strain ranging from 7 to 9% in the proximal aorta of the adult. However, these studies did not evaluate longitudinal strain after TEVAR. To our knowledge, the impact of TEVAR on longitudinal strain has not yet been reported.

Another main finding was that the thoracic porcine aortas were most prone to rupture in the longitudinal axis ($P < 0.001$), in particular in the proximal zone close to the arch ($P = 0.01$). This new finding may yield insight into the pathogenesis of TEVAR-related complications, such as retrograde dissection that typically occurs at the proximal end of a stent-graft.

Our observations are clinically relevant as they suggest that TEVAR causes acute segmental stiffening, which may increase wall stress in the adjacent segments [3]. Several authors proposed that such locally altered stress between the stent-graft and the aortic wall may be responsible for severe TEVAR-related complications such as retrograde dissection, stent-graft induced new entry-tear, aneurysm formation, rupture, endoleaks and stent-graft fractures and infolding [3–5, 21]. Our results showed a significant mismatch of longitudinal strain between the stented and non-stented aortic segments after TEVAR (Fig. 5). Such a mismatch may lead to the following mechanisms:

(i) Repetitive pulsatile friction between the stent-graft and the aortic wall, at both the proximal and distal end, which may cause traumatic lesions to the aortic wall or the stent-graft [21].
(ii) Increased wall stress along aortic segments adjacent to the stent-graft, at both the proximal and distal end, because of an increased impedance due to the stiffened stented segments [3].

Furthermore, we found that the strain mismatch between the stented and non-stented segments enlarged with rising pressure, potentially increasing the risk of aortic dissection and aneurysmal dilatation. This finding might have implications for clinical practice as it stresses the importance of strict blood pressure control in patients treated with TEVAR to minimize the strain mismatch. This supports the suggestion of others that perioperative hypertensive episodes might increase the risk of retrograde dissection after TEVAR [22], in particular in dissected aortas due to a weakened aortic wall.

During each cardiac cycle, the heart pulls the proximal aorta downwards, forcing it to stretch longitudinally [16, 20]. Stiffening of the descending thoracic aorta after TEVAR seems to limit this stretch, causing an increase in *in vivo* longitudinal strain in the segments proximal to the device (unpublished data). *In vivo*, the thoraco-abdominal aorta is proximally fixed to the heart, the supra-aortic vessels and the ligamentum arteriosum, and distally to the visceral arteries and the iliac bifurcation. Such a double-ended fixation forces the total thoraco-abdominal aorta to extend similarly before and after TEVAR. In our experimental set-up, the aortas were also double-ended fixed and prestretched; however, the distal end was allowed some freedom to be able to extend. As a result, we observed a shorter total aortic length after TEVAR when compared with before TEVAR (at 180 mmHg: 268.2 vs 280.3 mm, $P < 0.001$). This might explain why we did not observe an increase of longitudinal strain in the adjacent segments in this study. Further *in vivo* imaging studies are warranted to investigate changes in strain in segments adjacent to stent-grafts.

Uniaxial tensile testing showed that peak stress-to-rupture was lower for the longitudinal than for the circumferential fragments. These data support the study of Khanafer *et al.* [15]. But surprisingly, we also observed that longitudinal aortic tissue was more prone to rupture in the proximal zone than distally, while this was not the case for circumferential tissue (Fig. 2). This new finding implies that thoracic aortic tissue is more vulnerable for an acute increase of longitudinal wall stress than circumferential wall stress, in particular in proximal segments. This observation may clarify why most intimal tears are circumferentially orientated, as this is most likely the result of longitudinal intima failure [15, 16], and might indicate vulnerability of the proximal descending aorta.

Stent-graft oversizing did not determine the magnitude of longitudinal strain reduction, in our set-up. Nevertheless, we did observe a trend of increased longitudinal stiffening and severe oversizing (Table 2). Such aortic stiffening after severe oversizing might support the observation of Sincos *et al.* [8] who showed that device oversizing increased the risk of rupture. However, further studies are warranted to investigate the association between oversizing, longitudinal stiffening and rupture.

Stent-graft induced aortic stiffening as demonstrated by our experiments, is likely to have negative systemic effects since aortic stiffness is an established predictor of cardiovascular mortality [9, 11]. Acute aortic stiffening is also associated with important histological vascular wall changes, such as increased collagen-to-elastin ratio, with elevated risk of cardiovascular disease [3, 10]. Therefore, stent-graft induced stiffening may actually be considered as extremely accelerated ageing of the cardiovascular system, leading to acute aortic stiffening and increased cardiac afterload. These findings suggest that current stiff stent-grafts might be more harmful on the long-term than currently realized. In particular extensive stent-graft coverage might, hypothetically, have a profound impact. It may therefore be advisable to minimize the length of stent-graft coverage, if possible, to decrease adverse cardiovascular effects. However, this remains to be elucidated.

To improve long-term outcomes of aortic disease, we suggest that future studies should focus on the pathophysiology of TEVAR associated complications as well as on development of more elastic stent-grafts. Large *in vivo* studies using dynamic imaging, such as electrocardiogram-gated computed tomography or magnetic resonance imaging, are required to clarify the association between TEVAR and cardiovascular remodelling. However, such *in vivo* imaging studies on the highly pulsatile thoracic aorta are associated with out-of-plane motions and cardiac/respiratory artefacts [20, 23]. Therefore, we aimed to first assess the impact of TEVAR on longitudinal strain in a controlled experimental set-up, avoiding artefacts and allowing for aortic tissue marking to overcome out-of-plane motions.

It is reasonable to assume that more elastic stent-grafts might reduce aortic stiffening, adverse cardiovascular remodelling and strain mismatches, with potential favourable long-term outcomes. Currently, stent-grafts with longitudinal connection bars are designed to be stiff in the longitudinal axis to offer better fixation through the spring-back effect. However, it is exactly this spring-back force that might induce bird-beaking and the formation of intimal tears [4, 5]. Longitudinally, more elastic stent-graft designs with less spring-back force, dedicated to aortic dissection, should be considered. A first modification of the Medtronic stent-grafts was the elimination of the longitudinal connecting bar from the earlier design (Medtronic Talent), which was thought to be responsible for longitudinal stiffness and the spring-back effect. However, on the basis of this study, further longitudinal elasticity might be advised for future stent-graft designs to better fit the compliant aorta, with the aim of improving clinical outcomes in patients managed with TEVAR.

Study limitations

We acknowledge that the use of porcine aortas is an important limitation of this study. Nonetheless, porcine aortas are regularly used in cardiovascular research [19, 24], since their mechanical properties are comparable with those of young humans, and because they are much more widely available than human cadaveric samples. But, a porcine aorta is certainly more elastic than a diseased, often atherosclerotic, adult human aorta. However, we were not able to find data on longitudinal strain in diseased, degenerative, calcified human aortas. Moreover, we have so far not found a reproducible technique to modify the mechanical properties of aortic specimens that addresses the *in vivo* elastic modulus of aged diseased human aortas properly. Therefore, care should be taken when translating our results to the clinical practice. Further research focused on *in vivo* imaging studies of diseased adult aortas is necessary to make the step from the laboratory to clinic. Second, we used a non-pulsatile mock circulatory system, which allowed for a highly controllable experimental setting for our study purpose. However, we acknowledge that with this non-pulsatile set-up, we neglected inertial effects of pulse waves, which might have led to underestimation of *in vivo* strain. Nevertheless, experimental non-pulsatile mock circulatory models have widely shown to provide a valid strategy for the initial investigation of novel concepts regarding aortic elasticity [25]. Moreover, our observed strain rates were comparable with pulsatile *ex vivo* experimental data and *in vivo* patient data [19, 20].

Another drawback in this experimental study was the use of non-thrombotic blood analogue. Circulating a thrombotic agent, however, rapidly leads to clotting since there are no epithelial cells to inhibit this. Therefore, just like other *ex vivo* haemodynamic studies [19, 24], we used water, which sufficed for our main goal; imposing a stable intraluminal pressure. In addition, non-thrombotic fluid does not have relevant influence on the high-speed condition of the aorta [26].

It must also be noted that our findings only apply for Medtronic Valiant stent-grafts, which have interrupted stents. Other stent-graft designs, such as those with continuous stents, might show different rates of longitudinal strain. However, this was out of

scope for this study, which primarily focused on a first quantification of the impact of TEVAR on longitudinal strain. Lastly, our data on longitudinal strain in the segments adjacent to the stent-graft may not totally represent the *in vivo* condition. After all, the *in vivo* aortas are fixed by multiple elastic side branches, which most likely have a different impact on the adjacent segments than the fixations in our *ex vivo* set-up. Future *in vivo* studies are therefore warranted to further elucidate dynamic changes of the total thoracic aorta following TEVAR.

CONCLUSION

Our experimental study found that TEVAR acutely stiffened the thoracic aorta in the longitudinal direction. This resulted in a longitudinal strain mismatch between stented and non-stented segments. Uniaxial tensile testing demonstrated that thoracic aortic tissue is more prone to rupture in the longitudinal than the circumferential direction, in particular close to the arch. Such an acute strain mismatch of potentially vulnerable tissue might play a role in TEVAR-related complications, including retrograde dissection and aneurysm formation. The finding that TEVAR stiffens the aorta longitudinally may shed light on systemic complications following TEVAR, such as hypertension and cardiac remodelling. This initial study on the impact of TEVAR on longitudinal strain may serve as a base for future investigation on the interaction between aortic stent-grafts and cardiovascular biomechanics and might contribute to future stent-graft design.

SUPPLEMENTARY MATERIAL

Supplementary material is available at *EJCTS* online.

Funding

This work was supported by Ministero dell'Istruzione, dell'Università e della Ricerca [grant number 2010BFXRHS]; European Research Council Starting Grant through the Project ISOBIO: Isogeometric Methods for Biomechanics [grant number 259229]; iCardioCloud project by Cariplo Foundation [grant number 2013-1779] and Lombardy Region [grant number 42938382; grant number. 46554874].

Conflict of interest: none declared.

REFERENCES

[1] von Allmen RS, Anjum A, Powell JT. Incidence of descending aortic pathology and evaluation of the impact of thoracic endovascular aortic repair: a population-based study in England and Wales from 1999 to 2010. Eur J Vasc Endovasc Surg 2013;45:154–9.
[2] Tzilalis VD, Kamvysis D, Panagou P, Kaskarelis I, Lazarides MK, Perdikides T *et al.* Increased pulse wave velocity and arterial hypertension in young patients with thoracic aortic endografts. Ann Vasc Surg 2012;26:462–7.
[3] Raaz U, Zöllner AM, Schellinger IN, Toh R, Nakagami F, Brandt M *et al.* Segmental aortic stiffening contributes to experimental abdominal aortic aneurysm development. Circulation 2015;131:1783–95.
[4] Dong ZH, Fu WG, Wang YQ, Guo DQ, Xu X, Ji Y *et al.* Retrograde type A aortic dissection after endovascular stent graft placement for treatment of type B dissection. Circulation 2009;119:735–41.
[5] Dong Z, Fu W, Wang Y, Wang C, Yan Z, Guo D *et al.* Stent graft-induced new entry after endovascular repair for Stanford type B aortic dissection. J Vasc Surg 2010;52:1450–7.
[6] Kleinstreuer C, Li Z, Basciano CA, Seelecke S, Farber MA. Computational mechanics of Nitinol stent grafts. J Biomech 2008;41:2370–8.
[7] Tremblay D, Zigras T, Cartier R, Leduc L, Butany J, Mongrain R *et al.* A comparison of mechanical properties of materials used in aortic arch reconstruction. Ann Thorac Surg 2009;88:1484–91.
[8] Sincos IR, Aun R, da Silva ES, Belczak S, de Lourdes Higuchi M, Gornati VC *et al.* Impact of stent-graft oversizing on the thoracic aorta: experimental study in a porcine model. J Endovasc Ther 2011;18:576–84.
[9] Cavalcante JL, Lima JAC, Redheuil A, Al-Mallah MH. Aortic stiffness: current understanding and future directions. J Am Coll Cardiol 2011;57:1511–22.
[10] Dart AM, Kingwell BA. Pulse pressure—a review of mechanisms and clinical relevance. J Am Coll Cardiol 2001;37:975–84.
[11] Redheuil A, Wu CO, Kachenoura N, Ohyama Y, Yan RT, Bertoni AG *et al.* Proximal aortic distensibility is an independent predictor of all-cause mortality and incident CV events: the MESA study. J Am Coll Cardiol 2014;64:2619–29.
[12] Kingwell BA, Waddell TK, Medley TL, Cameron JD, Dart AM. Large artery stiffness predicts ischemic threshold in patients with coronary artery disease. J Am Coll Cardiol 2002;40:773–9.
[13] Takeda Y, Sakata Y, Ohtani T, Tamaki S, Omori Y, Tsukamoto Y *et al.* Endovascular aortic repair increases vascular stiffness and alters cardiac structure and function. Circ J 2014;78:322–8.
[14] Brekken R, Dahl T, Hernes TAN, Myhre HO. Reduced strain in abdominal aortic aneurysms after endovascular repair. J Endovasc Ther 2008;15:453–61.
[15] Khanafer K, Duprey A, Zainal M, Schlicht M, Williams D, Berguer R. Determination of the elastic modulus of ascending thoracic aortic aneurysm at different ranges of pressure using uniaxial tensile testing. J Thorac Cardiovasc Surg 2011;142:682–6.
[16] Beller CJ, Labrosse MR, Thubrikar MJ, Robicsek F. Role of aortic root motion in the pathogenesis of aortic dissection. Circulation 2004;109:763–9.
[17] Robich MP, Hagberg R, Schermerhorn ML, Pomposelli FB, Nilson MC, Gendron ML *et al.* Hypothermia severely effects performance of nitinol-based endovascular grafts in vitro. Ann Thorac Surg 2012;93:1223–7.
[18] Hannon JP, Bossone CA, Wade CE. Normal physiological values for conscious pigs used in biomedical research. Lab Anim Sci 1990;40:293–8.
[19] Krüger T, Grigoraviciute A, Veseli K, Schibilsky D, Wendel HP, Schneider W *et al.* Elastic properties of the young aorta: ex vivo perfusion experiments in a porcine model. Eur J Cardiothorac Surg 2015;48:221–7.
[20] Bell V, Mitchell WA, Sigurðsson S, Westenberg JJM, Gotal JD, Torjesen AA *et al.* Longitudinal and circumferential strain of the proximal aorta. J Am Heart Assoc 2014;3:e001536.
[21] Prasad A, To LK, Gorrepati ML, Zarins CK, Figueroa CA. Computational analysis of stresses acting on intermodular junctions in thoracic aortic endografts. J Endovasc Ther 2011;18:559–68.
[22] Khoynezhad A, White RA. Pathogenesis and management of retrograde type A aortic dissection after thoracic endovascular aortic repair. Ann Vasc Surg 2013;27:1201–6.
[23] Klinke V, Muzzarelli S, Lauriers N, Locca D, Vincenti G, Monney P *et al.* Quality assessment of cardiovascular magnetic resonance in the setting of the European CMR registry: description and validation of standardized criteria. J Cardiovasc Magn Reson 2013;15:55.
[24] Qing K-X, Chan YC, Lau SF, Yiu W-K, Ting ACW, Cheng SWK. Ex-vivo haemodynamic models for the study of Stanford type B aortic dissection in isolated porcine aorta. Eur J Vasc Endovasc Surg 2012;44:399–405.
[25] Lopata RGP, Peters MFJ, Nijs J, Oomens CWJ, Rutten MCM, van de Vosse FN. Vascular elastography: a validation study. Ultrasound Med Biol 2014;40:1882–95.
[26] Liu X, Fan Y, Deng X, Zhan F. Effect of non-Newtonian and pulsatile blood flow on mass transport in the human aorta. J Biomech 2011;44:1123–31.